Proceeding of the IEEE
International Conference on Robotics and Biomimetics
Dali, China, December 2019

Dynamic Obstacle Avoidance Planning for Manipulators of Home

Zhimin He, Fu Yuan, and Diansheng Chen* Member, IEEE, Min Wang

Robot Institute, School of Mechanical Engineering and Automation
Beihang University
Beijing, China

18813007802@163.com

***Abstract*— With the maturity of robotics and serious aging situation, home service robots have been prevailing around the world, which requires the robotic arm of home service robots to be flexible for obstacle avoidance to work in complex and changing home environment. Based on the actual requirements of home service robots, this paper proposes an obstacle avoidance planning algorithm based on improved artificial potential field method for dynamic obstacle avoidance of redundant manipulators. The velocity of the target object and obstacle were introduced into the end-planned field structure to plan a collision-free path for the end of the arm and track the dynamic target point. Meanwhile, the deviation speed of the arm member in the obstacle repulsive field was added to ensure obstacle avoidance. Finally, the effectiveness of the algorithm was verified in the simulation environment.**

I. INTRODUCTION

In 1959, the first industrial robot was born in the United States. In the following 60 years, robotics developed rapidly and new research directions and fields were continuously explored. From the industrial robots on the original factory automation production line to the sweeping robots that gradually entered the home, and then the Chang'e 4 rover to achieve the first lunar back landing, robots are everywhere in modern life. Home service robot is a special robot that can partially replace human beings to complete home service work. With the improvement of people's living standards and the wide application of artificial intelligence technology in the field of robotics, home service robots have gradually become one of the research central issue in the field of robotics. According to statistics from the International Federation of Robotics IFR in 2014, the global sales of home service robots has reached 4.7 million units, an increase of 28% over 2013[1]. Mr. Bill Gates, chairman of Microsoft, once said that the world will have "robots in every family"[2]. Home service robots have entered the family field and have become a major trend with their development.

However, the home environment is complex and changeable, which requires the robotic arm of the home service robot to be able to flexibly avoid obstacles in dynamic environment and smoothly complete the operations of grasping and controlling. In order to solve the problem of dynamic obstacle avoidance of mechanical arms, domestic and foreign scholars have done a lot of research. In 1983, Lazona-Perze from MIT proposed a C-space-based obstacle avoidance algorithm[3]. In 2013, ZHAO Dean's research team succeeded in using this method to achieve obstacle avoidance planning for robotic arms[4].Wang Juanjuan and others improved the grid method and obtained the shortest path of required precision by equally decreasing grid, which solved the problem of small grid application area[5]. Oussama Khatib proposed a virtual force method in 1986, namely the artificial potential field method[6]. Vadakkepat used a combination of genetic algorithm and artificial potential field method to plan an optimal path [7]. Sun Shaojie and others from the Ordnance Engineering College optimized the random escape algorithm by combining the equipotential line escape method with the random escape method[8]. After entering the 21st century, due to the rapid development of artificial intelligence, many intelligent planning algorithms have emerged. In 2000, Kindel et al. successfully introduced the probability road map method into the dynamic environment to avoid obstacles[9]. In 2010, Fragkopoulos et al. proposed a two-way random search tree algorithm, which generates a random tree from the C space starting point and the target point of the robot arm, which greatly shortens the time for establishing the search tree[10]. In 2014, Kai Jiang et al. proposed a fuzzy programming algorithm based on hierarchical control [11]. In 2014, S Aditya Gautam et al. proposed a planning method based on neural network algorithm and genetic algorithm, which can realize obstacle avoidance in robot 3D environment[12]. In 2016, Yun Chao et al. proposed an obstacle avoidance method based on radial basis function (RBF) neural network model and quadratic programming technology for the problem of motion flexibility of redundant manipulators and successfully realized the determination of the optimal configuration in the process of obstacle avoidance[13]. In 2014, Shen Haoyu et al. of Nanjing University of Aeronautics and Astronautics proposed a redundant mechanical arm obstacle avoidance algorithm based on master-slave task transformation, which successfully solved the problem of failure avoidance

*Resrach supported by the National Key R&D Program of China(2018YFB1307103).

Zhimin He is with the Robot institute, School of Mechanical Engineering and Automation, Beihang University, Beijing, 100191, China. (e-mail: 18813007802@163.com).

Fu Yuan is with the Robot institute, School of Mechanical Engineering and Automation, Beihang University, Beijing, 100191, China. (e-mail: yuanfu@buaa.edu.cn).

Diansheng Chen is with the Robot institute, School of Mechanical Engineering and Automation, Beihang University, Beijing, 100191, China. (corresponding author, phone: +86-010-82339089, e-mail: chends@buaa.edu.cn).

Min Wang is with the department of Academic Affairs Office, Beihang University, Beijing, 100191, China. (e-mail: wmin@buaa.edu.com).

978-1-7281-6321-5/19//$31.00 ©2019 IEEE

function of homogeneous solution when the obstacle is on the end trajectory[14].

Aiming at the redundant manipulator of the home service robot (DOF $\geqslant 7$), this paper proposes a dynamic obstacle avoidance algorithm based on improved artificial potential field method. The velocity of the target object and obstacle were introduced into the end-planned field structure to plan a collision-free path for the end of the arm and track the dynamic target point; and add the deviation speed to the arm member in the obstacle repulsive field to ensure obstacle avoidance.

II. KINEMATICS MODEL OF MANIPULATOR

The kinematics problem of the manipulator refers to the conversion relationship between the end position and the joint angle of the manipulator, including the two parts of the forward and reverse kinematics. Positive kinematics is the process of knowing the angular position of each joint of the mechanical arm and solving the three-dimensional position and attitude of the end. Inverse kinematics is the opposite.

A. Positive kinematics model

The redundant mechanical arm used in this paper is the 7-DOF robot arm lwa3 of the Schunk company. It is modeled according to the standard D-H method as shown in Fig. 1, the D-H parameters of each link are shown in Table 1.

Table 1 Robot arm D-H parameters

Link	α_i/°	a_i/mm	θ_i/°	d_i/mm
1	0	0	θ_1	L1
2	-90	0	θ_2	0
3	90	0	θ_3	L2
4	-90	0	θ_4	0
5	90	0	θ_5	L3
6	-90	0	θ_6	0
7	90	0	θ_7	0

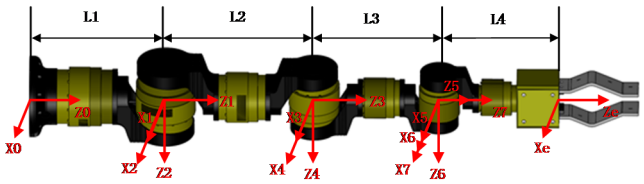

Fig 1. Robotic arm D-H modeling

The coordinate transformation relationship between two adjacent links is:

$$ {}^{i-1}_{i}T = \begin{bmatrix} \cos\theta_i & -\sin\theta_i\cos\alpha_i & \sin\theta_i\sin\alpha_i & a_i\cos\theta_i \\ \sin\theta_i & \cos\theta_i\cos\alpha_i & -\cos\theta_i\sin\alpha_i & a_i\sin\theta_i \\ 0 & \sin\alpha_i & \cos\alpha_i & d_i \\ 0 & 0 & 0 & 1 \end{bmatrix} \tag{1} $$

Among them, α_i、a_i、θ_i、d_i are a set of D-H parameters, (i=1,2，…，7). For rotating joints, α_i、a_i、d_i are constant, θ_i is variable. By sequentially multiplying the matrix (1), the transformation matrix of the end-of-arm coordinate system to the base coordinate system can be obtained (2):

$$ {}^{0}_{n}T = {}^{0}_{1}T{}^{1}_{2}T{}^{2}_{3}T \cdots {}^{n-1}_{n}T \tag{2} $$

Where n is the number of joints of the manipulator. This is the positive kinematics model of the manipulator.

B. Inverse kinematics solution

In this paper, the pseudo-inverse method is used to solve the inverse kinematics of the manipulator. At the same time, the pseudo-inverse method is easy to make the robot arm singularly heterogeneous. The problem is solved by the damped least squares method to improve the stability of the inverse kinematics algorithm.

In robotics, the mapping from Cartesian space to joint space is usually achieved by a Jacobian matrix, which maps the joint velocity to the generalized Cartesian velocity at the end of the manipulator, satisfying the following relationship.

$$ \dot{X} = J(\theta)\dot{\theta} \tag{3} $$

Among them, $\dot{X} = [v_x, v_y, v_z, \omega_x, \omega_y, \omega_z]^T$ indicates the generalized speed of the end of the arm in the workspace.$\dot{\theta} = [\dot{\theta}_1, \dot{\theta}_2, \dot{\theta}_3, \dot{\theta}_4, \dot{\theta}_5, \dot{\theta}_6, \dot{\theta}_7]^T$ is the joint angular velocity. $J(\theta)$ is a partial derivative matrix of θ, which is the Jacobian matrix of the manipulator, reflecting the relationship between the angular velocity of each joint of the robot arm and the generalized velocity of the end.

Pseudo-inverse method is a numerical solution to solve the inverse solution of mechanical arm from the speed level. The basic algorithm idea is: given the end position of the mechanical arm X_0 and the target pose X_n, plan the trajectory from the initial pose to the target pose in the joint space, and then calculate the generalized speed $\dot{X}$ of the end motion according to the trajectory point. According to the speed Jacobian formula $\dot{X} = J(\theta)\dot{\theta}$, the joint angular velocity $\dot{\theta}$ is obtained, and finally the angular velocity is integrated to obtain the joint angle value θ. However, since the redundant mechanical arm velocity Jacobian matrix is not a square matrix, it is impossible to solve $\dot{\theta}$ by direct inversion operation. Therefore, the inverse matrix is replaced by the pseudo inverse Jacobian matrix. The solution is:

$$ \dot{\theta} = J^{+}\dot{X} \tag{4} $$

Among them, $J^{+} = J^{T}(JJ^{T})^{-1}$ called the generalized inverse of the Jacobian matrix, also called pseudo-inverse.

In the process of using a single pseudo-inverse method, it will be found that the pseudo-inverse matrix J^{+}reaches infinity in the singular isomer of the robot arm, resulting in the problem that the obtained joint angular velocity is infinite. Damping-based least squares method can solve the above problems perfectly. The improved method is: by adding the damping coefficient λ to the optimization objective function (4) to slow the joint speed of the singular isomer of the mechanical arm to approach the infinity speed. And the improved expression is:

$$ \dot{\theta} = J^{T}(JJ^{T} + \lambda^{2}I)^{-1}\dot{X} \tag{5} $$

Where I is an m×m-dimensional unit array. The value of the damping coefficient λ is as follows:

$$\lambda^2 = \begin{cases} \lambda_0^2(1-\sigma_m/\sigma_0)^2 & \sigma_m < \sigma_0 \\ 0 & \sigma_m \geq \sigma_0 \end{cases} \quad (6)$$

Among them, σ_0 is the minimum critical singular value of the manipulator, and σ_m is the minimum singular value of the Jacobian matrix. It can be obtained by singular value decomposition of the Jacobian matrix, and λ_0 is the maximum damping coefficient.

III. DYNAMIC OBSTACLE AVOIDANCE ALGORITHM

There are actually two problems to be solved considering the obstacle avoidance of the manipulator. One is the trajectory planning at the end of the manipulator, that is, the obstacle avoidance at the end; the other is the obstacle avoidance of the mechanical arm member.For the first problem, the trajectory planning of the end of the manipulator, an improved artificial potential field method was proposed, which introduces the velocity of the target object and obstacle into the end-potential field construction, and plans a collision-free trajectory for the end and track dynamic target points. For the second problem, the obstacle avoidance of the mechanical arm member uses an additional speed deviation method based on the master-slave task transition to balance the problem between the mechanical arm obstacle avoidance and the end trajectory tracking.

A. Improved artificial potential field method

The artificial potential field method was first proposed by Oussama Khatib in 1986 and applied to the planning of mechanical arm obstacle avoidance paths.

Based on the traditional artificial potential field method, this paper introduces the velocity of the target point and the obstacle as parameters into the force field function, reconstructs the attractive field and the repulsive force field, and realizes tracking of the dynamic target point and avoidance of dynamic obstacles.

1) Improvement of the gravitational field

In the traditional artificial potential field method, the gravitational force at the end of the arm is only related to the distance to the target points. When the target point is stationary, the gravitational field is constructed in a way that fully satisfies the requirements. However, when the target point moves, the gravitational force generated by the traditional gravitational field is not strong enough to attract the end of arm keeping track of the target point. In order to solve this problem, this paper will add two parameters of the speed of the target point and the end speed of the arm in the traditional gravitational field construction function to improve the tracking performance.

Fig. 2 shows the schematic diagram of the attraction of the improved gravitational field to the end. In the figure, P_{goal} indicates the position of the target point, P_{tool} indicates the position of the end of the arm, V_{goal} indicates the speed of the target point, and V_{tool} indicates the current speed of the end of the arm. F_{pos} indicates the attractive force due to the distance between the end and the target point, F_{vel}indicates the attractive force due to the speed difference between the end and the target point, and F_{att} indicates the resultant force of the above two attractive forces. The end P_{tool} will get closer to the target point P_{goal} faster by the attraction force. Among them, the expressions of F_{pos} and F_{vel} are as follows:

$$F_{pos} = k_{pos} \cdot \left\| P_{goal} - P_{tool} \right\| \cdot P_{tool}P_{goal} / \left\| P_{tool}P_{goal} \right\| \quad (7)$$

$$F_{vel} = k_{vel} \cdot (V_{goal} - V_{tool}) \quad (8)$$

Where k_{pos} andk_{vel} represent the position force coefficient and the speed force coefficient, respectively, for controlling the speed of the end of the arm close to the target point.

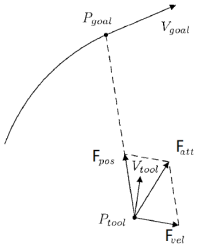

Fig 2. Improvement of gravity

2) Improvement of the repulsion field

Similarly, the obstacle velocity and the end velocity are introduced into the repulsive force field, as shown in Fig. 3.

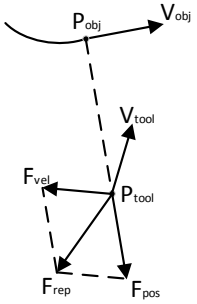

Fig 3. Improvement of the repulsive force

When the end of the arm enters the repulsion field of the obstacle, P_{obj} indicates the position of the obstacle (the repulsion source), P_{tool} indicates the position of the end of the arm, V_{obj} indicates the speed of the obstacle, and V_{tool} indicates the current speed of the end of the arm. F_{pos} indicates the repulsive force due to the distance between the end and the obstacle, F_{vel} indicates the repulsive force due to the speed difference between the end and the obstacle, and F_{att} indicates the resultant force of the above two repulsive forces. The end P_{tool} will move away from the obstacleP_{obj} faster under the action of the repulsive force, and escape the range of the repulsive force field. Among them, F_{pos} and F_{vel} are piecewise functions, and the expressions are as follows:

$$F_{pos} = \begin{cases} k_{pos}\left(\frac{1}{\left\| P_{obj}P_{tool} \right\|} - \frac{1}{\rho_0}\right)\frac{P_{obj}P_{tool}}{\left\| P_{obj}P_{tool} \right\|} & \left\| P_{obj}P_{tool} \right\| \leq \rho_0 \\ 0 & \left\| P_{obj}P_{tool} \right\| > \rho_0 \end{cases} \quad (9)$$

$$F_{vel} = \begin{cases} k_{vel}\left(\frac{1}{\left\|P_{obj}P_{tool}\right\|}-\frac{1}{\rho_v}\right)\frac{V_{goal}-V_{tool}}{\left\|V_{goal}-V_{tool}\right\|} & \left\|P_{obj}P_{tool}\right\| \le \rho_v \\ 0 & \left\|P_{obj}P_{tool}\right\| > \rho_v \end{cases} \tag{10}$$

Among them, k_{pos} and k_{vel} respectively represent the position force coefficient and the speed force coefficient of the repulsive force, which are used to control the speed of the end escaping from the repulsive field. $\left\|P_{obj}P_{tool}\right\|$ indicates the distance between the obstacle and the end; ρ_0 indicates the radius of the repulsive field based on the position; ρ_v indicates the radius of the repulsive field based on the velocity.

B. Additional speed deviation method based on master-slave task conversion

1) Speed deviation method

The speed deviation method is a method proposed by Klein A.C for obstacle avoidance of redundant mechanical arms. Since the joint space dimension of the redundant manipulator is larger than the dimension of the working space, the degree of freedom redundancy is generated. Therefore, the redundant manipulator theoretically has numerous joint space solutions. The speed deviation method is to use a force that is away from the obstacle in the arm member to generate a deviation speed, and to obtain a solution that satisfies both the end trajectory requirement and the obstacle avoidance. In the inverse solution of the manipulator, the positive kinematics equation of the 7-DOF redundant manipulator is simultaneously differentiated to obtain the velocity equation.

$$\dot{X} = J(\theta)\dot{\theta} \tag{11}$$

Where $\dot{X} = [v_x, v_y, v_z, \omega_x, \omega_y, \omega_z]^T$, indicating the generalized velocity of the end of the arm in the workspace; $[\dot{\theta}_1, \dot{\theta}_2, \dot{\theta}_3, \dot{\theta}_4, \dot{\theta}_5, \dot{\theta}_6, \dot{\theta}_7]^T$ representing the joint angular velocity; J (θ) is the partial derivative matrix of θ, namely, the Jacobian matrix of the arm that reflects the relationship between the angular velocity of each joint of the robot arm and the generalized velocity of the tip.

For the redundant manipulator, there is no conventional inverse solution for the Jacobian matrix, only the generalized inverse solution. By solving the generalized inverse of the Jacobian matrix, we can get, the solution of nonlinear equations $\dot{\theta}$ consists of the general solution of the homogeneous equations $\dot{\theta_h}$ and the special solution of non-zero terms $\dot{\theta_s}$:

$$\dot{\theta} = \dot{\theta_h} + \dot{\theta_s} = (I - J^+J)v + J^+\dot{X} \tag{12}$$

Where J^+ represents the generalized inverse of the mechanical arm Jacobian matrix; I represents the unit matrix of the same dimension as J^+J, which is a 7×7 unit matrix in this paper; v represents an arbitrary vector in the joint space. Since $(I - J^+J)$ is a projection in the zero space of the Jacobian matrix, $J(I - J^+J)$=0, so v can take arbitrary value in the joint space. For convenience, usually $N = (I - J^+J)$, then the formula (12) is simplified to:

$$\dot{\theta} = Nv + J^+\dot{X} \tag{13}$$

Fig. 4 is a schematic diagram of the application of the speed deviation method applied in obstacle avoidance of redundant manipulator. First a safety distance d_m is set. When the distance between the manipulator and the closest point of obstacle(A_0) $d_0 < d_m$, the speed deviation method is used to exert a speed $\dot{X}_0$ so that the arm goes away from obstacle.

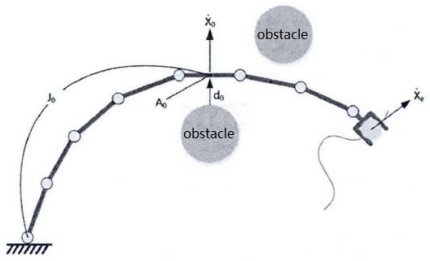

Fig 4. Schematic diagram of the speed deviation method

The joint velocity produced by the deviation speed $\dot{X}_0$ can be solved by equation (14):

$$\dot{X}_0 = J_0\dot{\theta} \tag{14}$$

Where J_0 is the Jacobian matrix at point A_0 which can be obtained by equation (13) and (14):

$$\dot{\theta} = J^+\dot{X} + (J_0N)^+(\dot{X}_0 - J_0J^+\dot{X}) \tag{15}$$

The above is an inverse kinematic solution equation for the redundant manipulator using the velocity deviation method for a single obstacle. The first term $J^+\dot{X}$ on the right side of the equation is a special solution component, indicating the end of the arm to track the target. The second term $(J_0N)^+(\dot{X}_0 - J_0J^+\dot{X})$ on the right side of the equation is a general solution component, indicating the obstacle avoidance of the arm member. At the same time, the value and direction of $\dot{X}_0$ determine the obstacle avoidance effect of the mechanical arm. Assuming that the maximum additional speed of the arm member is $\dot{X}_m$, the relationship between the obstacle avoidance speed $\dot{X}_0$ and the maximum obstacle avoidance speed is as follows:

$$\dot{X}_0 = \alpha\dot{X}_m \tag{16}$$

Where α is the obstacle avoidance speed coefficient, 0⩽α⩽1, and its expression is as follows:

$$\alpha = \begin{cases} -\sin(\pi d_0/2d_m) + 1 & d_0 < d_m \\ 0 & d_0 \ge d_m \end{cases} \tag{17}$$

Where d_0 is the closest distance of the manipulator to the obstacle, and d_m is the safe distance.

2) Master-slave task conversion algorithm

With additional deviation speeds, most obstacle avoidance problems of redundant robotic arms can be solve. However, in some special positions, the robotic arm cannot balance the main task target tracking and additional task obstacle avoidance. At this time, in order to better realize the safety motion control of the manipulator, it is necessary to limit the main task and improve the priority of the obstacle avoidance task. The resulting planning strategy is the master-slave task transformation method.

The algorithm of the master-slave task transformation method is: during the movement of the robot arm, when the arm

member is outside the obstacle safety zone, the preset planning algorithm is normally operated. When it enters the safety area of the obstacle, the adjustment is made to change the priority of target tracking task and obstacle avoidance task. The closer the distance between the obstacle and the manipulator, the higher the obstacle avoidance priority and the lower the target tracking priority, until the obstacle avoidance priority exceeds the target tracking priority, completing the main task and the additional task conversion.

In this paper, the speed deviation method and the master-slave task conversion method are synthesized by adding a priority coefficient β to the algorithm of the speed deviation algorithm expression (15). The expression after combining the two algorithms is as follows:

$$\dot{\theta} = (1-\beta)\cdot J^{+}\dot{X} + \beta\cdot(J_0 N)^{+}(\dot{X}_0 - J_0 J^{+}\dot{X}) \quad (18)$$

Where the expression of the priority coefficient β is as follows:

$$\beta = \begin{cases} 1 & d_0 < d_2 \\ 1+\cos(\pi(d_0+d_2)/2(d_1-d_2)) & d_2 \le d_0 < d_1 \\ 0 & d_0 \ge d_1 \end{cases} \quad (19)$$

Where d_0 represents the closest distance of the mechanical arm member to the obstacle, d_1 is the prohibited area radius, and d_1 is the safe area radius of the obstacle.

IV. Simulation and Verification

In order to verify the effectiveness of the redundant mechanical kinematics model and the improved artificial potential field method used in this paper, this chapter uses MATLAB software to simulate the actual mechanical arm system for simulation test.

A. Tracking dynamic targets

In order to verify the performance of the improved artificial potential field method for dynamic targets tracking in this chapter, this section will test without any obstacles in the robot arm workspace. The initial conditions of the test are: the initial joint angle of the arm is (0, π/2, 0, -π/2, 0, 0, 0), and the end of the arm is in the global coordinate system (-0.328, 0, 0.9137, 0, 0, 0). The initial position of the target point is set to (0, 0.15, 1.0), and the moving speed is (0, 0.2, 0). The above angle units are all rad, the angular velocity units are rad/s, the length units are m, and the speed units are m/s. Iterative calculation time interval T = 0.01 s.

The path of the end of the arm and the dynamic target point is shown in Fig. 5(a). The red circle in the figure represents the path of the end of the arm, and the blue is path of the target point. It can be seen that the end of the arm is gradually approaching the target point location during the planning process. From the figure, the trajectory tracking of the end to the target point can be more clearly seen. Fig. 5(b) is the distance curve between the end of the arm and the target point. It can be seen from the figure that the distance is gradually decreasing, which is in line with the expectation of the target tracking. Fig. 5(c) is the angle curve of the joint space, it can be seen that the joint angle motion is smooth. Fig. 5(d) shows the curve of joint angular velocity. It can be seen that the maximum joint angular velocity is less than 0.06 rad/s, which appears in the early stage of joint planning.

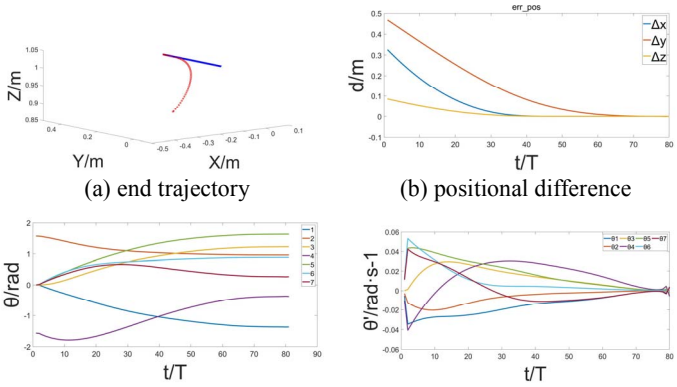

(a) end trajectory (b) positional difference

(c) angle change (d) angular velocity change

Fig 5. Dynamic target tracking

B. Dynamic obstacle avoidance

Next is the evasion verification of the robotic arm for dynamic obstacles. In order to eliminate the influence of dynamic target points on dynamic obstacle avoidance simulation analysis, the target point is set as a static target point. The initial joint angle of the arm is $(0, \frac{\pi}{2}, 0, -\frac{\pi}{2}, 0, 0, 0)$, and its end is in the global coordinate system (-0.328,0,0.9137,0,0,0). The initial position of the target point is set to (0.4, 0.4, 0.8) and left still, and the starting position of the three obstacles is (0.3, 0.2, 0.8; 0.1, 0.1, 0.8; -0.1, 0.1, 0.8). The obstacles are set to a uniform motion, and the speed of motion is (0.2, 0, 0; 0, 0.2, 0; 0, 0, 0.2). At the same time, the radius of the safety zone of the obstacle is 0.05m, and the radius of the safety zone of the arm is set to 0.05m. The above angle units are all rad, the angular velocity units are rad/s, the length units are m, and the speed units are m/s, iterative calculation time interval T=0.01s. The initial position of the arm, target point and obstacle is shown in Fig. 6(a), and the arrow in the figure indicates the direction of movement of the obstacle.

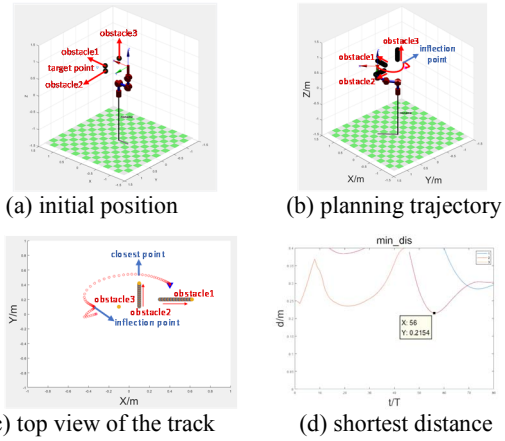

(a) initial position (b) planning trajectory

(c) top view of the track (d) shortest distance

Fig 6. Schematic diagram of dynamic obstacle avoidance

The path of the robot arm in the dynamic obstacle environment is shown in Fig. 6(b). Shortly after the start of the movement, there is an inflection point at the end of the arm. At

this time, the arm is affected by the movement of the obstacle 3 in the positive direction of the Z axis. Under the action of the improved repulsive force field, the obstacle is bypassed from the side and the arm continues to move towards the target point. From the top view of the trajectory shown in Fig. 6(c), the trajectory change at the inflection point can be more clearly seen. Then, under the obstacles of obstacle 1 and obstacle 2, the arm selects the outer ring to detour to the target point. The shortest distance between the robot arm and the three obstacles during the whole motion is shown in Fig. 6(d). It can be seen that the shortest distance during the movement is 0.2154m, which is greater than the sum of the radius of the safety zone of the robot arm and the obstacle($d_1 = 0.3m, d_2 = 0.1m$), which meets the obstacle avoidance requirement.

C. Comprehensive simulation

Finally, consider the situation where both the target point and the obstacle move. In this simulation, the starting position and obstacle position of the arm are the same as in the previous experiment. The initial position of the target point is set to (0.1, 0.4, 0.8), the target point motion speed is set to (0.2, 0, 0). The initial position of the robot arm, target point and obstacle is shown in Fig. 7(a), and the arrow in the figure indicates the moving direction of the target point and the obstacle.

From Fig.7(b), the tracking of dynamic target points and the avoidance of dynamic obstacles can be seen more clearly. Fig. 7(c) is the distance curve between the end of the arm and the target point. The space distance at the end point in the figure is less than 1mm. Fig. 7(d) is the shortest distance curve between the manipulator and three dynamic obstacles. The shortest distance in the figure is 0.1711m, which is greater than the sum of the radius of the safety zone of the robot arm and the obstacle ($d_1 = 0.3m, d_2 = 0.1m$).

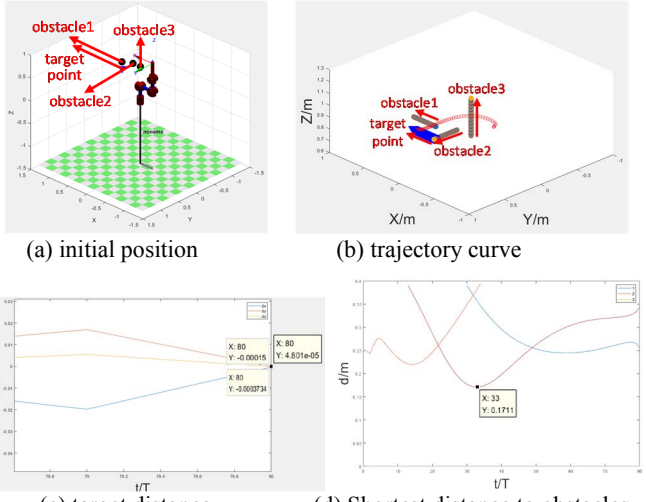

(a) initial position (b) trajectory curve

(c) target distance (d) Shortest distance to obstacles

Fig 7. Schematic diagram of comprehensive simulation

In summary, it can be considered that the improved obstacle avoidance algorithm can make the robot arm track the dynamic target point well in the dynamic environment while avoiding obstacles.

V. CONCLUSIONS

In this paper, for the redundant manipulator of the home service robot (DOF $\geqslant$ 7), the kinematics model is first established, and the inverse solution method is given. Then, according to the obstacle avoidance demand of the complex dynamic environment of the family, a dynamic obstacle avoidance algorithm based on the improved artificial potential field method is proposed. The velocity of the target object and obstacles is introduced into the end-potential field construction to plan a no collision path and track dynamic target points. At the same time, for the obstacle avoidance of the mechanical arm member, the additional speed deviation method based on the master-slave task conversion is used to balance the problem between the obstacle avoidance of the mechanical arm and the end tracking. Finally, the paper verifies the effectiveness and feasibility of the proposed algorithm by simulating the motion of the manipulator in MATLAB software.

REFERENCES

[1] Liang C. IFR released the latest global service robot statistical report [J]. Robotics Industry, 2016 (03): 33-36.

[2] Gaces B.A robot in every home[J].Scientific American, 2007, 296(1):58-65.

[3] Lozano-Perez, "Spatial Planning: A Configuration Space Approach". IEEE Transactions on Computers. 1983,32(2):108-120.

[4] ZHAO Dean, Lv Jidong, Ji Wei. Smoothing obstacle avoidance path planning based on C-space for harvesting robot[J]. Proceedings of the 32nd Chinese Control Conference, 2013: 5662-5666.

[5] Juanjuan W, Kai C. Robot Path Planning Based on Grid Method [J]. Agricultural Equipment and Vehicle Engineering, 2009(4): 14-17.

[6] Kondo K. Motion planning with six degrees of freedom by multistrategic bidirectional heuristic free-space enumeration[J]. IEEE Trans on Robotics and Automation, 1991, 7(3): 267-277.

[7] P Vadakkepat, TH. Lee, L. Xin. Application of evolutionary artificial potential field in robot soccer system[C] IFSA World Congress and 20th NAFIPS International Conference, 2001.Joint 9th IEEE,2001:2781-2785

[8] Shaojie S, Xiaohui Q, Lijun S, Cheng Z. Research on obstacle avoidance method of mechanical arm based on artificial potential field-genetic algorithm [J]. Computer Measurement and Control, 2011. 19(12): 3078-3081.

[9] R. Kindel, D. Hsu, JC. Latombe, S. Rock. Kinodynamic motion planning amidst moving obstacles[C].Robotics and Automation, 2000. Proceedings. ICRA IEEE International Conference on volumel .IEEE, 2000:537-543.

[10] C. Fragkopoulos, A. Graeser. A RRT based path planning algorithm for rehabilitation robots[C].International Symposium and German Conference on Robotics(ROBOTIK) VDE. 2010:1-8.

[11] Kai Jiang, Li Chungui. Path planning based on fuzzy logic algorithm for robots in hierarchical control[J]. International Conference on Machine Tool Technology and Mechatronics Engineering,ICMTTME 2014: 701-704.

[12] S Aditya Gautam, Nilmani Verma. Path planning for unmanned aerial vehicle based on genetic algorithm & artificial neural network in 3D[J]. 014 International Conference on Data Mining and Intelligent Computing, ICDMIC 2014: 1-5.

[13] Chao Y, Gang L, Gang W, Xuebing Y. Research on Obstacle Avoidance of Redundant Manipulators Based on RBF Neural Network and Quadratic Programming [J].Mechanical & Electrical Engineering,2016, 33(1): 1-7.

[14] Haoyu S, Hongtao W, Bai C, Li D, Xiaolong Y. Redundant robot obstacle avoidance algorithm based on master-slave task transformation [J]. Robot, 2014, 36(4): 425-429.